Mechanosynthesis of nanocrystalline ZrB$_2$-based powders by mechanically induced self-sustaining reaction method

M. Jalaly [1,*], M.Sh. Bafghi [1], M. Tamizifar [1], F.J. Gotor [2]

1. School of Metallurgy and Materials Engineering, Iran University of Science & Technology (IUST), Narmak, Tehran 16846-13114, Iran

2. Instituto de Ciencia de Materiales de Sevilla, Americo Vespucio 49, 41092 Sevilla, Spain

Corresponding Author, Email: maisam_jalaly@iust.ac.ir

Tel: +989127387902, Fax: +982177240480

Abstract

Preparation of nanocrystalline ZrB$_2$–based powder by aluminothermic and magnesiothermic reductions in M/ZrO$_2$/B$_2$O$_3$ (M = Al or Mg) systems was investigated. In this research, high energy ball milling was employed to persuade necessary conditions for the occurrence of a mechanically induced self-sustaining reaction (MSR). The happening of MSR reactions was recorded by a noticeable pressure rise in the system during milling. Ignition times for ZrB$_2$ formation by aluminothermic and magnesiothermic reductions were found to be 13 and 6 minutes, respectively. Zirconium diboride formation mechanism in both systems was explained through the analysis of the relevant sub-reactions.

Keywords: Zirconium diboride; Mechanosynthesis; Reaction mechanism; Ball milling

1. Introduction

Ultra-high temperature materials (UHTMs) are a group of materials that are chemically and physically stable at very high temperatures in extreme reactive environments. Several borides, carbides, and nitrides of group IV and V elements are

1

anticipated to be potentially suitable for such applications. All borides, carbides, and nitrides in this category have similar properties, such as high melting point and hardness due to the strong covalent bonding. However, the borides tend to have higher thermal conductivity compared to the carbides and nitrides, which gives them better thermal shock resistance.
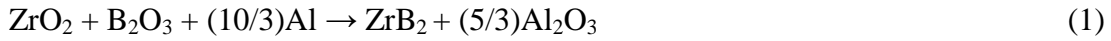
Diboride zirconium has been found to be a suitable material for high-temperature applications because of its excellent properties such as high melting point (greater than 3000°C), high hardness and strength at room and elevated temperatures, good thermal and electrical conductivities, low thermal expansion coefficients, chemical inertness, good oxidation resistance, and high thermal stability [1]. The distinctive features of these materials make them good selections to be employed in various applications from industrial applications such as cutting tools, wear resistant coatings, molten metal crucibles and high temperature electrodes to military ones such as hypersonic flights, atmospheric re-entry vehicles, and rocket propulsion systems. Among the borides, ZrB_2 and HfB_2 have attracted the most attention because of their superior oxidation resistance, which is a consequence of the stability of ZrO_2 and HfO_2 oxide formed on these materials at high temperatures in oxidizing atmospheres [2].

It is of great importance to select the proper method of synthesis because of its significant effect on the properties of the products. Zirconium diboride can be synthesized by various techniques including solid state methods, liquid state methods and gas state methods [3]. Solid state synthesis of ZrB_2 can be achieved through several different routes including the reaction of elemental Zr and B [1,4-6]; borothermic reduction of ZrO_2 [7,8]; carbothermic reduction of ZrO_2 and B_2O_3 [9,10]; reduction of ZrO_2 by boron carbide [11-13]; and metallothermic reduction of ZrO_2 and B_2O_3 [14-20].

Literature review [3] shows that metallothermic reduction route has been more interesting due to its cheaper raw material as well as the high exothermic nature of the involving self-sustainable reactions. Research works concerning the metallothermic process of ZrB_2 synthesis based on self-propagating high temperature synthesis (SHS) reactions have been performed by various methods, such as reactive hot pressing [6], arc resistive ignition [17], and high energy ball milling [10,16,20]. Highly exothermic chemical reactions can be induced by high energy ball milling leading to a self-sustaining reaction within the milling vial after the elapse of a critical milling period, called the ignition time. This kind of process, known as a mechanically induced self-sustaining reaction (MSR) [21], is similar to thermally ignited SHS systems. In contrast to the conventional SHS procedure, MSR process has the kinetically favorable side benefit of mixing of the reactants as well as the subsequent homogenization of the products together with their extremely particle size reduction in one single step [4]. Mechanically induced self-sustaining reaction processes are often accomplished at short times due to the instantaneous nature of involving SHS reactions.

ZrB_2 synthesis by use of high energy ball milling has been examined by a group of researchers. Setoudeh and Welham [16] studied ZrB_2 formation by conducting the magnesiothermic reduction reaction by milling, using ZrO_2 and B_2O_3 as Zr and B bearing source. In this study, no MSR process occurred and ZrB_2 was synthesized after 15 hours of milling which is comparable to a normal mechanical alloying. Akgun et al. [20] also attempted to produce zirconium diboride by mechanochmical treatment of ZrO_2-B_2O_3-Mg. Zirconium diboride has been obtained after 30 hours of milling in their effort.

3

Therefore, the intention of the present research work was to investigate the mechanosynthesis of ZrB_2 powder by use of ZrO_2 and B_2O_3 as starting material and application of mechanically induced self-sustaining reactions (MSR) of both alumino- and magnesiothermic reduction which has not been ever reported. The self-sustaining reactions are as follows:

$$ZrO_2 + B_2O_3 + (10/3)Al \rightarrow ZrB_2 + (5/3)Al_2O_3 \qquad (1)$$

$$\Delta G°_{298} = -722 \text{ kJ}, \ \Delta H°_{298} = -746 \text{ kJ}, \ T_{ad} \approx 2330 \text{ K}$$

$$ZrO_2 + B_2O_3 + 5Mg \rightarrow ZrB_2 + 5MgO \qquad (2)$$

$$\Delta G°_{298} = -931 \text{ kJ}, \ \Delta H°_{298} = -960 \text{ kJ}, \ T_{ad} \approx 2900 \text{ K}$$

2. Material and methods

The stoichiometric amounts of monoclinic ZrO_2 (99%, Aldrich, USA), B_2O_3 (98%, Fluka, USA), Al (99%, Aldrich, USA), and Mg (99%, Riedel-deHaen, Germany) powders were used as starting materials to synthesize ZrB_2. High energy ball milling was conducted in a planetary ball mill (Pulverisette7, Fritsch, Germany) at 600 RPM using a ball-to-powder mass ratio of 30:1. The milling vial and balls (15 mm) were made of hardened chromium steel. Milling experiments were performed under high-purity argon gas of 5bar pressure. The vial was purged with argon gas several times, and the determined pressure was adjusted before the start of the milling. The vial was connected to the gas cylinder during the milling experiments by a rotating union and a flexible polyamide tube. The pressure changes vs. time were monitored by a SMC solenoid valve (model EVT307-5DO-01F-Q, SMC Co,. Tokyo, Japan) to record the ignition occasion. Once the MSR reaction was occurring, a sharp peak emerged in this diagram due to the pressure rise resulted from temperature increase. The position of this

peak shows the ignition time. The system used in this work has already been shown elsewhere [22].

X-ray powder diffraction (XRD) analysis was performed to determine the structural changes of powder during milling experiments. A Panalitycal X'Pert diffractometer (45 kV, 40 mA) with Cu Kα radiation (λ=0.15406 nm) was used for XRD analysis. The XRD patterns were recorded in the 2θ range of 10–80° (step size 0.05° and time per step 1s). The crystallite sizes of samples were estimated by broadening analysis of XRD peaks using Williamson–Hall formula:

$$\frac{\beta}{2}\cot\theta = \frac{0.45\,\lambda}{\sin\theta\,D} + \varepsilon \tag{3}$$

where β is the peak breadth in mid height, θ is the Bragg diffraction angle, λ is the X-ray wave length, D is the average crystallite size and ε is the mean value of internal strain.

3. Results and Discussion

3.1. Aluminothermic reduction

Fig. 1 shows the variation of gas pressure inside the vial versus milling time in $Al/B_2O_3/ZrO_2$ system (reaction 1). A great pressure rise can be clearly observed at about 13 min milling representing a great exothermic reaction. It implies that the MSR reaction occurs at this point and the ignition time is around 13 min.

The XRD patterns of Al, ZrO_2 and B_2O_3 powder mixture as-received and after different milling times are shown in Fig. 2. The XRD pattern of as-received powder mixture included only the sharp peaks of Al (ICCD PDF #03-0932), ZrO_2 (ICCD PDF #13-0307) and B_2O_3 (ICCD PDF #06-0297). As can be seen the products of reaction (1), ZrB_2 (ICCD PDF #34-0423) and Al_2O_3 (ICCD PDF #11-0661), were completely developed with sharp peaks after 13 min milling, although traces of Al and ZrO_2 were

5

still observed. This is a typical behavior in mechanosynthesis reactions, especially in MSR systems [21], due to entrapment of some powders in dead zones of milling vial. With increasing the milling time, unprocessed powders gradually find the chance of being subjected to the ball incidences and gaining sufficient energy to be locally reacted. There was no peak in Fig.1 after 13 min indicating that the amount of unreacted agglomerates and/or entrapped particles is negligibly small. They can be locally ignited so that temperature and pressure do not sensibly rise. As seen in Fig. 2, a specific kind of ZrO_2 (designated as $T\text{-}ZrO_2$) has been detected among unreacted materials in the samples milled for 13 min (ignition point). Zirconium dioxide has normally a monoclinic crystal structure at room temperature. It transforms at high temperatures to tetragonal type. Hence, it seems that a portion of starting monoclinic zirconia has transformed to tetragonal one due to the great increase of temperature resulted from highly exothermic MSR reaction. As Fig. 2 shows, a very slight amount of elemental Zr can be recognized in the XRD pattern related to the sample after 13 min milling. The Fig. 2 shows the XRD patterns of samples milled for 1 and 2 hours. Although slight amounts of zirconium dioxide can be observed after 1 h milling, it is obvious that the peaks of remaining Al and ZrO_2 completely disappeared after 2 h milling. The corresponding peaks of ZrB_2 and Al_2O_3 were broadened and their intensity gradually reduced during long-term ball milling suggesting the introduction of lattice defects into the crystal structures and decreasing the grain size of the product into nanoscales. The crystallite size and internal strain of ZrB_2 after 2 h ball milling were calculated to be around 83 nm and 0.65 %, respectively. The mechanism of ZrB_2 formation in the present system can be explained as follows, where the main reaction seems to have the following three sub-reactions:

$$2Al + B_2O_3 \rightarrow 2B + Al_2O_3 \tag{4}$$

$$\Delta G^\circ_{298} = -389 \text{ kJ}, \ \Delta H^\circ_{298} = -404 \text{ kJ}, \ T_{ad} \approx 2310 \text{ K}$$

$$(4/3) \, Al + ZrO_2 \rightarrow Zr + (2/3) \, Al_2O_3 \tag{5}$$

$$\Delta G^\circ_{298} = -15 \text{ kJ}, \ \Delta H^\circ_{298} = -20 \text{ kJ}, \ T_{ad} \approx 500 \text{ K}$$

$$Zr + 2B \rightarrow ZrB_2 \tag{6}$$

$$\Delta G^\circ_{298} = -318 \text{ kJ}, \ \Delta H^\circ_{298} = -322 \text{ kJ}, \ T_{ad} \approx 3200 \text{ K}$$

Aluminum reduces boron oxide and zirconium oxide to form elemental boron and zirconium. ZrB_2 can be subsequently formed by the reaction between these two elements. With regard to the adiabatic temperatures (T_{ad}) of above equations, reactions 4 and 6 possess the necessary conditions to satisfy Merzhanov criterion [20] to proceed in an SHS manner. But, the reduction of ZrO_2 by Al (reaction 5) does not satisfy this condition, i.e. aluminum cannot thermodynamically reduce zirconia in an SHS manner. The reduction behavior of B_2O_3 and ZrO_2 by Al and Mg can be compared in the Ellingham diagram as shown in Fig. 3. It is seen from this diagram that Al-Al_2O_3 line approximately coincides that of Zr-ZrO_2, especially at low temperatures. Consequently, Al does not have the sufficient thermodynamic ability to dissociate zirconia. When Al, B_2O_3 and ZrO_2 are simultaneously present in the system, Al reduces boron oxide in an SHS manner to yield elemental boron together with the release of a giant amount of heat which increases the system temperature inside the milling vial to such a level which can trigger the reaction between Al and zirconia to form elemental Zr. Then, ZrB_2 can be synthesized by the reaction between these two elements. This approach can be confirmed by the presence of a slight amount of remaining elemental zirconium in the XRD pattern exactly after ignition time. Great negative values of ΔG° and ΔH° of the following reaction can provide further support for the mentioned mechanism.

$3ZrO_2 + 10B = 3ZrB_2 + 2B_2O_3$ (7)

$\Delta G^\circ_{298}= -221 \text{ kJ}, \ \Delta H^\circ_{298}= -219 \text{ kJ}, \ T_{ad} \approx 770 \text{ K}$

Thereafter, B_2O_3 produced in the above reaction reduces again with aluminum. All these reactions can occur instantaneously if a suitable condition is provided.

In order to examine the proposed mechanism, sub-reactions were studied. The MSR manner of the reaction between Zr and B has been already confirmed [1, 3] and hence, this sub-reaction was not dealt with again in the present work.

The stoichiometric amounts of Al/B_2O_3 and Al/ZrO_2 according to the reactions 4 and 5 were mixed and milled in the same conditions. For reaction 4, the ignition time obtained from the corresponding pressure-time curve (Fig. 1) was found to be about 25 min, which is longer than the ignition time of reaction 1 due to the lower exothermicity of reaction 4. Fig. 4(a) shows the XRD pattern of un-milled and milled $Al-B_2O_3$ powder mixtures. It can be seen that powder mixture after ignition included Al_2O_3 and a little remaining initial materials. Boron element cannot be observed in the pattern most likely due to its amorphization as a result of the high temperature rise and high cooling rate in the MSR reaction. For reaction 5, no pressure rise was observed during the long time of milling as expected from the Ellingham diagram (Fig. 3). Fig. 4(b) shows the XRD pattern of un-milled and milled $Al-ZrO_2$ powder mixtures until 4 h. It is evident that the only phenomenon is peak broadening of initial materials and no reaction occurred during the long time of milling, indicating that Al cannot individually reduce zirconia in this condition, as mentioned above, due to the very small enthalpy of reaction 5. Introduction of boron oxide to this system can motivate the decomposition of zirconia because of the addition of a great deal of heat to the system.

It should be pointed out that the product resulted from aluminothermic reduction is a composite of $ZrB_2–Al_2O_3$. Although Al_2O_3 can be removed by an appropriate NaOH leaching process [23], it should be studied in detail elsewhere. The principal aim of the present work has been the examination of the feasibility of MSR synthesis of ZrB_2 during high energy milling technique. Furthermore, there are some research works focused on the formation of diboride–alumina composites as attractive materials in some applications [18, 19, 24].

3.2. Magnesiothermic reduction

The change of internal pressure of vial versus milling time for the $Mg/B_2O_3/ZrO_2$ system (reaction 2) was shown in Fig. 1. The emergence of an enormous peak at about 6 min demonstrates the occurrence of an intense exothermic reaction. The much higher pressure rise which also happens sooner in the case of magnesiothermic reaction (reaction 2) compared to that of aluminothermic reaction (reaction 1) is a reasonable consequence of the fact that the former reaction is noticeably more vigorous than the latter one due to its higher heat generation capacity (enthalpy).

XRD patterns of initial mixture and milled samples are illustrated in Fig. 5. In the pattern related to initial powder mixture only the peaks of Mg (ICCD PDF #35-0821), ZrO_2 and B_2O_3 compounds can be seen. After the elapse of 6 minutes of milling (ignition time), the products of reaction 2, i.e. ZrB_2 and MgO (ICCD PDF #04-0829), have been completely formed, although some traces of Mg and ZrO_2 can be still observed. Local reactions between remaining materials can occur at the extended milling time. Fig. 5 shows the XRD pattern of samples milled for 2 and 3 h. The disappearance of the remaining compounds after 3 h milling is obvious. The crystallite

size of ZrB_2 after 3 h ball milling was calculated to be about 56 nm. The higher intensity of tetragonal ZrO_2 peaks after the ignition time in the magnesiothermic reduction system as compared to aluminothermic reduction can be attributed to higher exothermicity of the former reaction which causes a higher degree of zirconia transformation. The removal of the MgO by-product in magnesiothermic process is much easier than Al_2O_3 by-product in aluminothermic process. In order to purify the ZrB_2 product, dissolution of magnesium oxide by-product was performed by 1M HCl leaching at 80°C for 1 hour. The XRD pattern of a leached product which has been milled for 3 h, is shown in Fig. 5. As the figure shows, magnesium oxide has been completely removed and the major phase after leaching is ZrB_2 together with very small trace of unreacted ZrO_2 appearing by a small peak at about 31°. Slight remaining of ZrO_2 in various reactions, due to its high chemical stability, has been reported by several researchers [14, 16, 18].

ZrB_2 formation through magnesiothermic reduction is supposed to have a mechanism including three sub-reactions similar to that of aluminothermic reaction which was mentioned earlier. Here, three sub-reactions are as follows:

$$3Mg + B_2O_3 \rightarrow 2B + 3MgO \tag{8}$$

$\Delta G°_{298}= -515$ kJ, $\Delta H°_{298}= -532$ kJ, $T_{ad} \approx 2630$ K

$$2Mg + ZrO_2 \rightarrow Zr + 2MgO \tag{9}$$

$\Delta G°_{298}= -98$ kJ, $\Delta H°_{298}= -107$ kJ, $T_{ad} \approx 1070$ K

$$Zr + 2B \rightarrow ZrB_2 \tag{10}$$
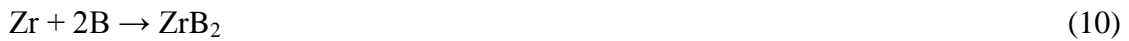
$\Delta G°_{298}= -318$ kJ, $\Delta H°_{298}= -322$ kJ, $T_{ad} \approx 3200$ K

Boron and zirconium elements should be reduced from their corresponding oxides by magnesium and combine to form zirconium diboride. The reaction between boron oxide

and Mg is a highly exothermic reaction with an SHS nature, while reduction of ZrO_2 by Mg (reaction 9) is an ordinary non-SHS reaction. Ellingham diagram (Fig. 3) shows a small difference between Mg-MgO and Zr-ZrO_2 lines. Although Mg is expected to be able to reduce zirconium dioxide from the thermodynamic standpoint, low adiabatic temperature of this reaction implies that it is not an SHS reaction and high temperatures or very long time are necessary for this reaction to take place. Under the circumstances like reaction 2 that Mg, ZrO_2 and B_2O_3 are simultaneously together, extreme amount of heat generated by the SHS reaction of Mg and B_2O_3 stimulates reduction of ZrO_2 to Zr. Highly exothermic reaction of the reduced components B and Zr (reaction 10) adds extra amounts of heat to the system resulting in the Zr reduction to proceed more easily.

To show the possibility of magnisiothermic reduction of B_2O_3 and ZrO_2 separately, stoichiometric amounts of Mg/B_2O_3 and Mg/ZrO_2 in accordance to reactions 8 and 9 were mixed and milled for the appropriate time durations. The ignition time of reaction 8 was found to be around 8 min (see Fig. 1), which is a little longer than that of reaction 2 (6 min) whose reason is believed to be the less heat generation of former reaction compared to the latter one. XRD pattern of initial material along with that of the sample milled up to the ignition point (8 min) are shown in Fig. 6(a). It can be seen in this figure that ignited sample contains magnesium oxide product together with small amounts of the starting materials. Boron element cannot be observed in the pattern most likely due to its glassy state. Small amounts of a MgO-rich spinel (3MgO.B_2O_3) has also been formed after ignition as XRD results show. This kind of spinel phase is supposed to be formed as a consequence of the reaction between higher amounts of MgO as the reaction product and lower amounts of the remaining boron oxide. For reaction 9, as expected from its thermodynamic data, no pressure rise was observed

11

throughout the milling time. Fig. 6(b) shows the XRD pattern of un-milled and milled powders up to 4 h in this system. There is only peak broadening of initial materials with no sign of the occurrence of any reaction during this long time. This indicates that Mg cannot reduce zirconia under the prevailed conditions. This reaction might happen by gradual mutual diffusion of materials under the extremely intensive conditions for much longer time.

4. Conclusion

High energy ball milling technique was successfully applied to mechanosynthesize nanocrystalline ZrB_2 by use of Al and Mg as the reducing agents. Synthesis in both $Al/B_2O_3/ZrO_2$ and $Mg/B_2O_3/ZrO_2$ found to have SHS nature with ignition times of 13 and 6 min, respectively. Examination of the sub-reactions revealed that boron oxide is easily reduced by both Al and Mg, while none of these two reductants can reduce ZrO_2 to Zr in an SHS manner. It has been concluded that the great heat generated through the reduction of boron oxide by either Al or Mg together with the large amount of heat released by the reaction between the reduced B and Zr is capable of activating the reduction of ZrO_2. Magnesiothermic reduction seems to be more attractive compared to aluminothermic one, since MgO can be much more easily removed through dissolution.

References

[1] M.A. Aviles, J.M. Cordoba, M.J. Sayagues, F.J. Gotor, Mechanochemical synthesis of $Ti_{1-x}Zr_xB_2$ and $Ti_{1-x}Hf_xB_2$ solid solutions, Ceramics International 37 (2011) 1895–1904.

[2] W.G. Fahrenholtz, G.E. Hilmas, Refractory Diborides of Zirconium and Hafnium, Journal of the American Ceramic Society 90 (2007) 1347–1364.

[3] J. K. Sonber, A. K. Suri, Synthesis and consolidation of zirconium diboride: review, Advances in Applied Ceramics 110 (2011) 321-334.

[4] M.A. Aviles, J.M. Cordoba, M.J. Sayagues, M.D. Alcala, F.J. Gotor, Mechanosynthesis of $Hf_{1-x}Zr_xB_2$ solid solution and $Hf_{1-x}Zr_xB_2$/SiC composite powders, Journal of the American Ceramic Society 93 (2010) 696–702.

[5] H.E. Camurlu, F. Maglia, Preparation of nano-size ZrB2 powder by self-propagating high-temperature synthesis, Journal of the European Ceramic Society 29 (2009) 1501–1506.

[6] A.L. Chamberlain, W.G. Fahrenholtz, G.E. Hilmas, Reactive hot pressing of zirconium diboride, Journal of the European Ceramic Society 29 (2009) 3401–3408.

[7] P. Peshev, G. Bliznakov, On the borothermic preparation of titanium, zirconium and hafnium diborides, Journal of the Less-common metals 14 (1968) 23-32.

[8] S.Ran, O. Van der Biest, J. Vleugels, ZrB_2 Powders Synthesis by Borothermal Reduction, Journal of the American Ceramic Society 93 (2010) 1586–1590.

[9] A.K. Khanra, L.C. Pathak, M.M. Godkhindi, Carbothermal synthesis of zirconium diboride (ZrB_2) whiskers, Advances in Applied Ceramics 106 (2007) 155–160.

[10] O. Balc, D. Agaogullar, I. Duman, M.L. Ovecoglu, Carbothermal production of ZrB_2–ZrO_2 ceramic powders from ZrO_2–B_2O_3/B system by high-energy ball milling and annealing assisted process, Ceramics International 38 (2012) 2201–2207.

[11] H. Zhao, Y. He, Z. Jin, Preparation of Zirconium Boride Powder, Journal of the American Ceramic Society 78 (1995) 2534–2536.

[12] J.K. Sonber, T.S.R. Ch. Murthy, C. Subramanian, S. Kumar, R.K. Fotedar, A.K. Suri, Investigations on synthesis of ZrB_2 and development of new composites with HfB_2 and $TiSi_2$, International Journal of Refractory Metals and Hard Materials 29 (2011) 21–30.

[13] W.M. Guo, G.J. Zhang, Reaction Processes and Characterization of ZrB_2 Powder Prepared by Boro/Carbothermal Reduction of ZrO_2 in Vacuum, Journal of the American Ceramic Society 92 (2009) 264–267.

[14] A.K. Khanra, L.C. Pathak, S.K. Mishra, M.M. Godkhindi, Sintering of ultrafine zirconium diboride powder prepared by modified SHS technique, Advances in Applied Ceramics 104 (2005) 282–284.

[15] K. Nishiyama, T. Nakamur, S. Utsumi, H. Sakai, M. Abe, Preparation of ultrafine boride powders by metallothermic reduction method, Journal of Physics: Conference Series 176 (2009) 012043.

[16] N. Setoudeh, N.J. Welham, Formation of zirconium diboride (ZrB_2) by room temperature mechanochemical reaction between ZrO_2, B_2O_3 and Mg, Journal of Alloys and Compounds 420 (2006) 225–228.

[17] S.K. Mishra, S. Das, L.C. Pathak, Defect structures in zirconium diboride powder prepared by self-propagating high-temperature synthesis, Materials Science and Engineering A364 (2004) 249–255.

[18] S.K. Mishra, S.K. Das, V. Sherbacov, Fabrication of Al_2O_3–ZrB_2 in situ composite by SHS dynamic compaction: A novel approach, Composites Science and Technology 67 (2007) 2447–2453.

[19] Y.B. Lee, H.C. Park, K.D. Oh, C.R. Bowen, R. Stevens, Self-propagating high-temperature synthesis of ZrB_2 in the system ZrO_2-B_2O_3-Fe_2O_3-Al, Journal of Materials Science Letters 19 (2000) 469– 471.

[20] B. Akgun, H.E. Camurlu, Y. Topkaya, N. Sevinc, Mechanochemical and volume combustion synthesis of ZrB_2, International Journal of Refractory Metals and Hard Materials 29 (2011) 601–607.

[21] L. Takacs, Self-sustaining reactions induced by ball milling, Progress in Materials Science 47 (2002) 355–414.

[22] F.J. Gotor, M. Achimovicova, C. Real, P. Balaz, Influence of the milling parameters on the mechanical work intensity in planetary mills, Powder Technology 233 (2013) 1–7.

[23] S. Sarkar, The removal of alumina and silica from iron rejects slime by chemical leaching, Hydrometallurgy 105 (2011) 364–369.

[24] J. Liu, P.D. Ownby, Enhanced mechanical properties of alumina by dispersed titanium diboride particulate inclusions, Journal of the American Ceramic Society 74 (1991) 241–243.
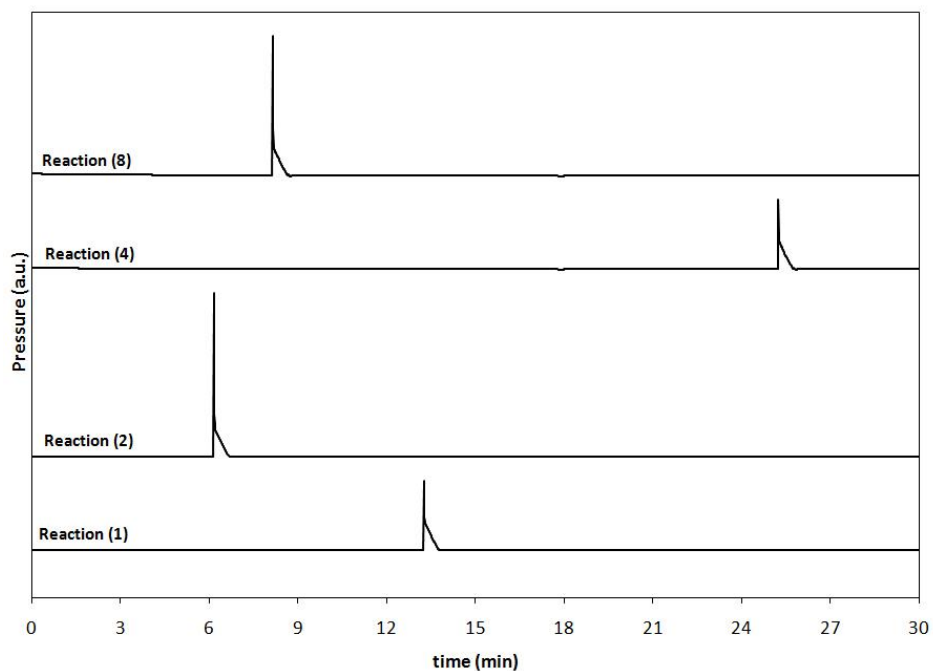
Fig. 1. The change of the pressure inside the vial versus milling time due to the occurrence of

self-sustaining ignition in different systems.
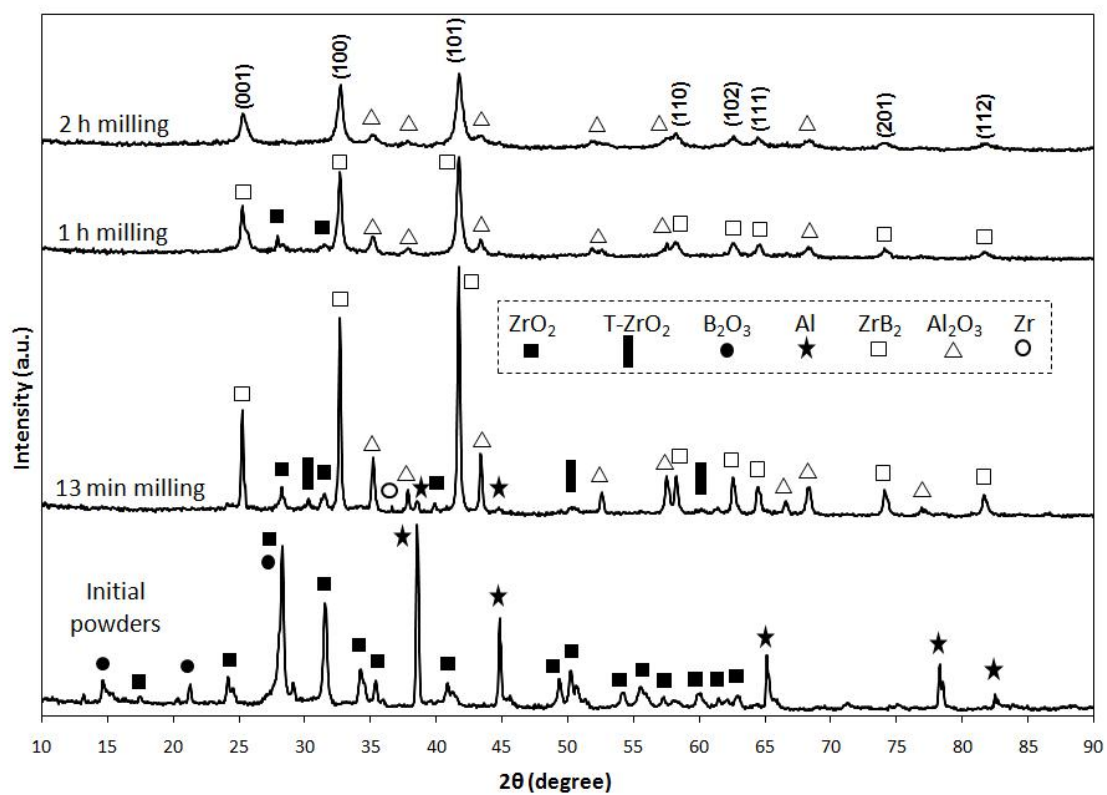
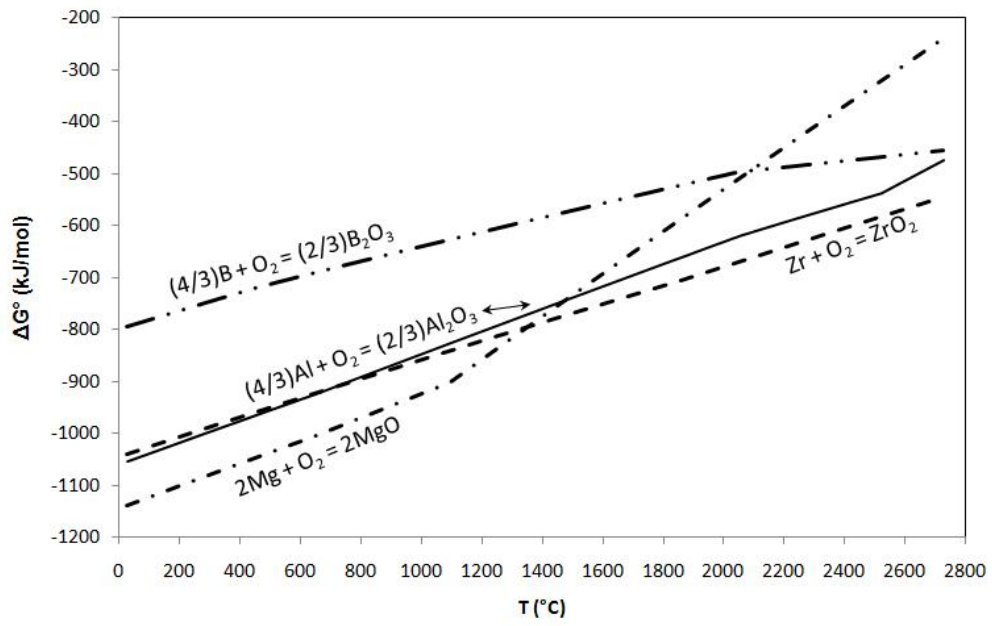Fig. 2. X-ray diffraction patterns of as-received and as-milled samples of Al/ZrO$_2$/B$_2$O$_3$ system.

Fig. 3. Ellingham diagram of Mg-MgO, Zr-ZrO$_2$, Al-Al$_2$O$_3$ and B-B$_2$O$_3$ systems.
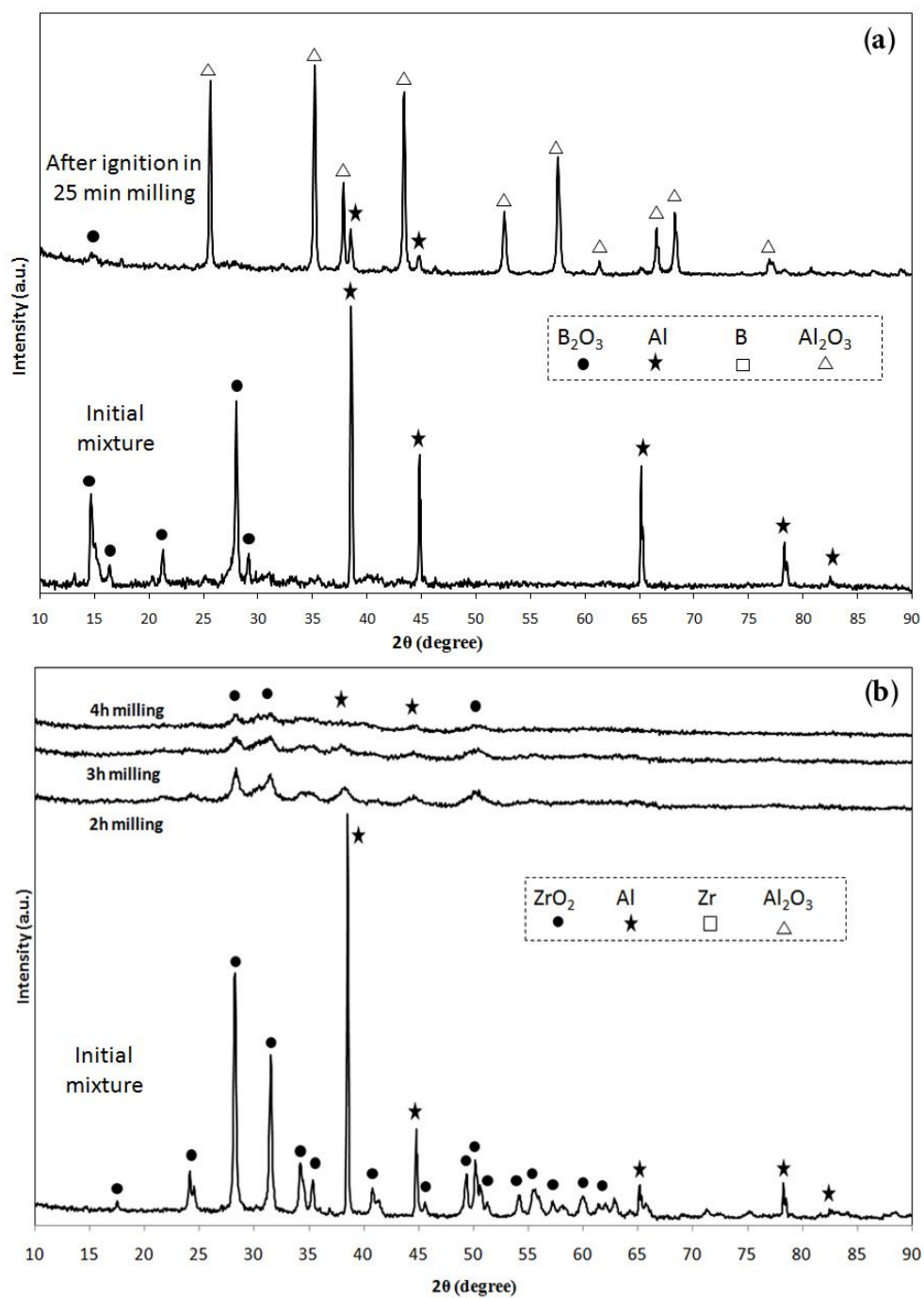
Fig. 4. X-ray diffraction patterns of initial and as-milled samples in (a) Al/B$_2$O$_3$ and (b) Al/ZrO$_2$

systems. The MSR reaction occurred in (a), but no ignition was observed in (b).
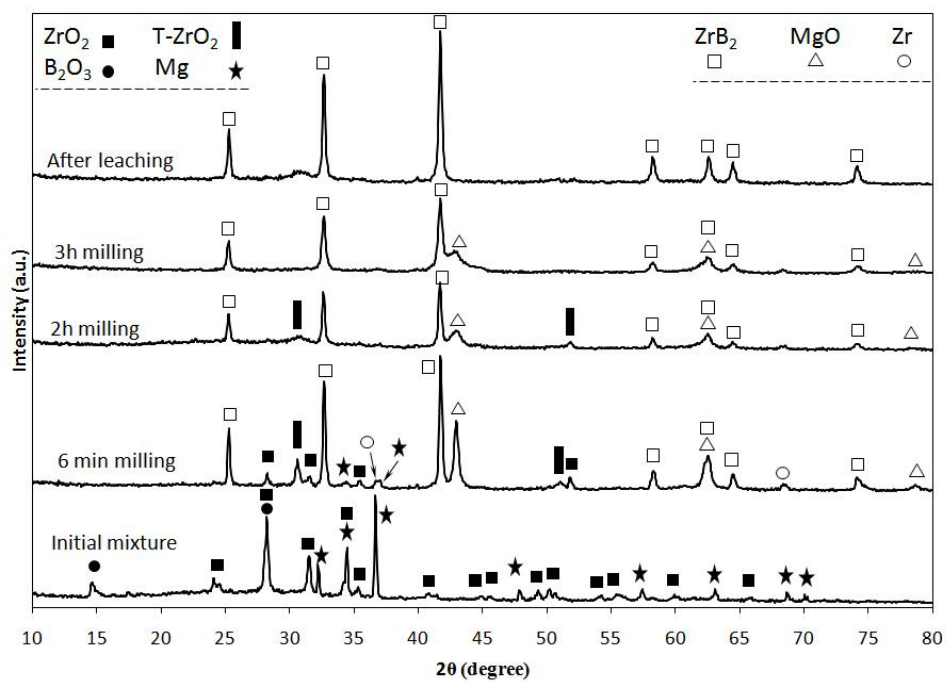
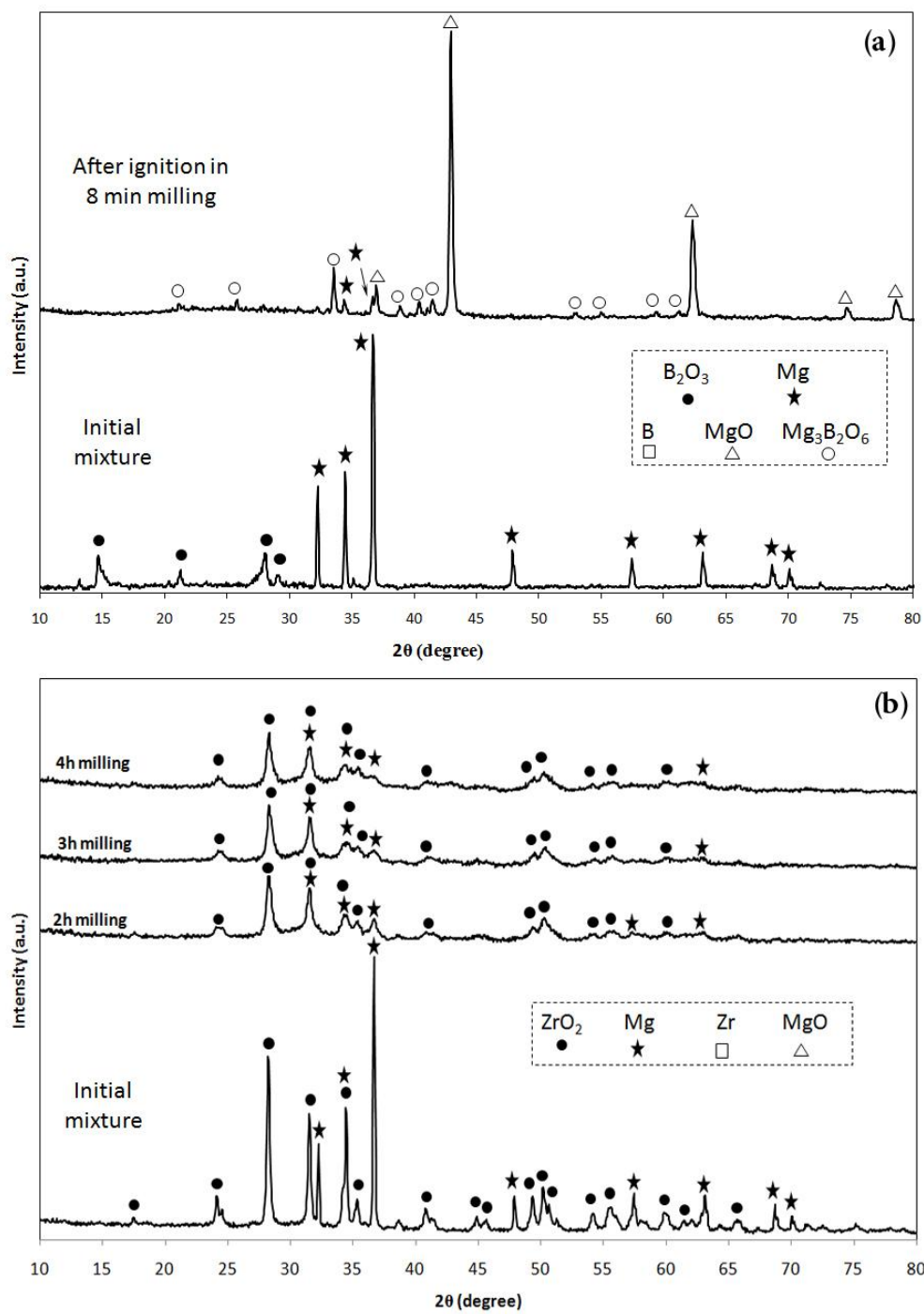Fig. 5. X-ray diffraction patterns of as-received and as-milled samples of $Mg/ZrO_2/B_2O_3$ system.

Fig. 6. X-ray diffraction patterns of as-received and as-milled samples in (a) Mg/B_2O_3 and (b) Mg/ZrO_2 systems. The MSR reaction occurred in (a), but no ignition was observed in (b).